

## MICROMECHANICAL INVESTIGATION AND PHENOMENOLOGICAL MODELING OF AL-8090 SUPERPLASTIC MATERIALS

H. Garmestani, P. N. Kalu and F. Boeshaghi

FAMU-FSU College of Engineering, Department of Mechanical Engineering  
& Center for Materials Research and Technology (MARTECH)  
Tallahassee, Florida 32310-2175

### ABSTRACT

In spite of its great technological importance, our understanding of the phenomenon of superplasticity is incomplete in several critical respects. It is believed that superplasticity occurs as a result of grain boundary sliding which results in changes in microstructure and reduction of texture. However, there is a reoccurring controversy over the accommodation mechanisms which facilitates the process and its interaction with grain boundary sliding. Recent advances in electron microscopy methods have improved the ability to analyze the microstructure of deformed materials. This paper presents the results obtained primarily from the application of one of such techniques, Orientation Imaging Microscopy (OIM), in the study of microstructural evolution in superplastically deformed Al-Li materials. The OIM technique incorporates automatic analysis of electron backscattered diffraction patterns with precise movement of a computer-controlled stage to produce accurate measurement of lattice orientation. The data can be reconstructed to produce grain boundary maps, which is a form of microstructure representation. The analysis of these maps revealed the complexity of the processes involved in the formation of high and low angle boundaries in superplastic materials. An attempt was made to correlate these misorientation data to the mechanical response of the superplastic material through a phenomenologically based model.

### INTRODUCTION

Superplasticity refers to the ability of some materials to deform to exceptionally large strains at elevated temperatures. Conventional superplastic forming (SPF) takes place at intermediate strain rate (approximately  $10^{-4} \text{ s}^{-1}$ ), and elongations as high as 4850% are not uncommon [1, 2]. This remarkable mechanical response has been attributed to high sensitivity of flow stress to strain rate and the principal prerequisite for the phenomenon is a fine, equiaxed grain size. It is commonly accepted that grain boundary sliding (GBS) is the dominant mechanism of SPF. The strain compatibility during SPF is maintained by concurrent accommodation process which may involve grain boundary migration, diffusion or dislocation motion. Grain boundary sliding is postulated as a unit step and the accommodation is considered to be rate controlling [3-7]. Such a mechanistic separation of GBS and the accommodation process resulted in the development of models which primarily rely on the accommodation process to drive the rate equations. Although in Ball and Hutchinson's model [8], GBS was not restricted to individual grains, the formulation did not seem to use this fact very effectively. Mukherjee later introduced a modified version of the model which restricted the GBS to individual grains [9]. The results of his experiments showed that GBS is localized in boundaries between domains of grains. This realization can clarify and improve the nature of the modeling efforts. This procedure provided us with the ground work for a phenomenologically based model which is based on the microstructure in which a dynamic process of grain boundary sliding and matrix deformation (dislocation climb and glide, diffusional creep,...) can occur simultaneously at all regions of the microstructure (Figure 1). Hart developed a purely mechanistic model in 1967 [10] which can be used to predict the three regions of strain rates for superplastic materials. The model was based on the assumption that there are regions in the matrix which slide through a Newtonian viscous process while the rest of the matrix accommodate the strain incompatibility generated due to slip. The model is phenomenological and all parameters can be determined from experiments such as strain rate change and load relaxation. In Hart's formulation, the material constants are assumed to be a

function of the microstructure. It was suggested that extensive research is needed to make such a correlation. Baudelet [11] extended Hart's formulation by incorporating the diffusional controlled process of Ashby-Verrall's model to account for the low strain rate transition. Although the model preserved the main features of the original Hart's model, it still cannot predict the high and very low strain rate regions of log stress - log strain rate curve. Therefore, there is still a need to produce a comprehensive model that will account for deformation over the entire range of strain rate. An attempt has been made in this study to produce a modified Hart's Model which accounts for the entire deformation range. Also, a relationship between the material constants and the microstructural parameters has been established.

#### MODIFIED HART'S MODEL (MHM)

Similar to other models, the MHM is based on considering grain boundary sliding (GBS) as the main mechanism of superplastic deformation, which is accommodated by other mechanisms (slip, glide and climb) in order to satisfy compatibility. Grain boundary sliding is represented through a Newtonian viscous process. The parameters are only dependent on grain size,  $d$ , and temperature,  $T$ . Specific to this model is the dependence to dislocation density through a hardness parameter called  $\sigma^*$ . The interrelation among the different parameters can be represented in a Maxwell type model. We present a uniaxial version of the full model as represented in Figure 1 [12], where  $\sigma$  and  $\dot{\epsilon}$  are the total stress and strain rates. The subscripts  $s$  and  $m$  designate the stress and strain rates associated with the matrix and grain boundary sliding. The full equations are presented in the following:

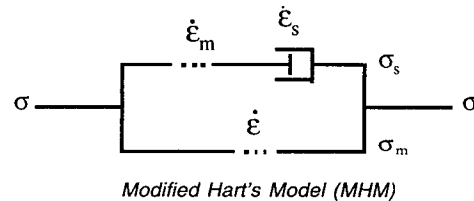


Figure 1. The rheological models

$$\sigma = y\sigma_s + (1-y)\sigma_m \quad (1)$$

$$\dot{\epsilon} = \dot{\epsilon}_s + \dot{\epsilon}_m \quad (2)$$

$$\ln \sigma_m = \ln \sigma^* - \left( \frac{\dot{\epsilon}^*}{\dot{\epsilon}} \right)^\lambda \quad (3)$$

$$\dot{\epsilon}^* = \left( \frac{\sigma^*}{G} \right)^m f \exp\left(-\frac{Q}{RT}\right)$$

$$\sigma_s = A \frac{kT}{\delta D_g} \left( \frac{d}{b} \right)^p \dot{\epsilon}_s \quad (4)$$

$$\dot{\epsilon} = \dot{a}^* \left( \frac{\sigma - \sigma^*}{G} \right)^M \quad (5)$$

where,  $d$  is the grain size,  $\delta$ , the grain boundary width,  $D_g$ , the grain boundary diffusion coefficient,  $\sigma^*$ , the dislocation density hardness parameter,  $p$ , the grain size exponent which is usually around 2-3, and  $\epsilon_s$  and  $\epsilon_m$  are assumed to have equal weights. The parameter  $y$  is a function of the area fraction of the sliding region. It can be determined phenomenologically using the experimental data and compared to the grain size distribution for different misorientation angles. In order to obtain these parameters a detailed microstructural characterization is necessary. A graphical representation of the individual mechanisms of the proposed rheology and their composite behavior is illustrated (Figure 2).

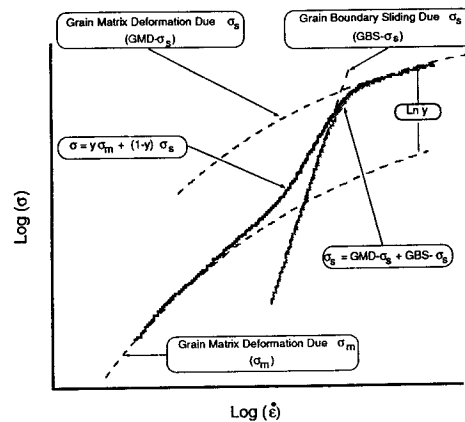


Figure 2- Strain rate s flow stress prediction of MHM model

### CHARACTERIZATION OF SUPERPLASTIC MATERIALS

The technique used for grain boundary characterization is Orientation Imaging Microscopy (OIM). Electron backscattered pattern (EBSP) in Scanning Electron Microscope (SEM) has grown to become an accepted technique in orientation measurement of polycrystalline materials in which the grains are larger than one micron [7, 13]. The automation of this technique, Orientation Imaging Microscopy (OIM), provides an on-line analysis of the diffraction patterns [9, 14]. Here, the EBSP's are collected from points on the sample surface over a regular grid and then automatically indexed. From this data, a map, called an OIM micrograph, is constructed displaying changes in crystal orientation over the specimen surface. In the OIM micrograph, the orientation of each point in the microstructure is known and hence the location, length and misorientation of all boundaries. This information is used to construct a micrograph based on a criteria input by the investigator. For a detailed analysis of this technique refer to [15].

To investigate the evolution of the microstructure based on the grain boundary misorientation distribution, a set of Al-8090 specimens were deformed at 516 °C and at a rate of  $10^{-4} \text{ sec}^{-1}$  to different strains. Figure 3-a is the image quality (IQ) micrograph for a sample deformed to 15%. The microstructure is essentially equiaxed and similar to that obtained by conventional optical or scanning electron microscopy techniques. Figure 3-b is an OIM image constructed using the same data set as in Figure 3-a but drawn to reveal boundaries with misorientation between  $1^\circ$  and  $10^\circ$  as thin lines, and those boundaries with misorientation greater than  $10^\circ$  as thick lines. The microstructure appears to be equiaxed. When boundaries with misorientations greater than  $10^\circ$  are plotted, the microstructure consists of fine grains sandwiched between coarse grain structures (Figure 4-a). The corresponding EBSP pole figures obtained from these grains are shown in Figure 4-b. It is clear that the microstructure exhibits a rotated cube type texture with three distinct pole segments, A, B and C corresponding to the three grains A, B and C in Figure 4-a.

One of the parameters which can be extracted from the microstructure is  $y$ , where  $y$  can be assumed to be the volume (or area) fraction of the sliding region. Grain boundary sliding is expected to occur at high angle grain boundaries. The major task is then to identify the high angle grain boundaries. Traditionally, high angle boundaries are expected to be 15 degrees or more. The exact nature of such a definition is not very clear.

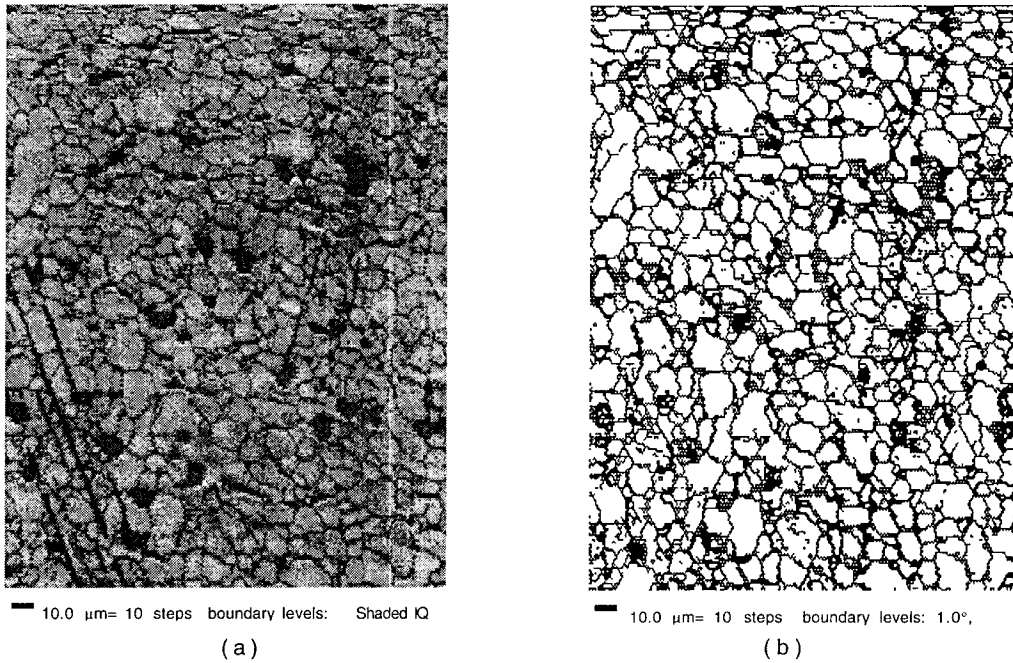


Figure 3- a) Image Quality (IQ) micrograph and b) Misorientation boundary micrograph- Thin and thick lines represent grain boundaries with misorientation greater than  $1^\circ$  and greater than  $10^\circ$  respectively. Al-8090 specimen deformed to 15% strain.

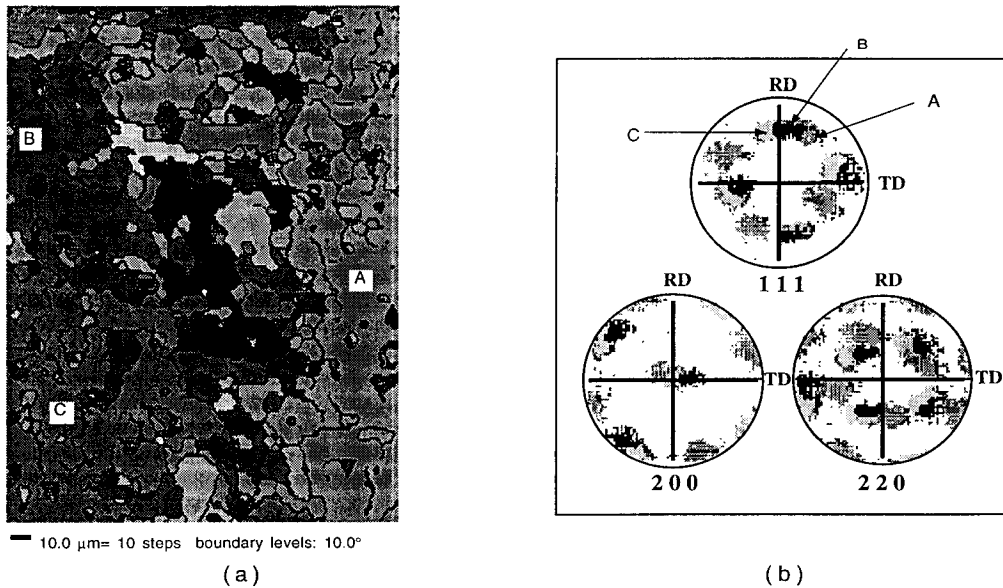


Figure 4- (a)  $10^\circ$  Misorientation boundary micrographs. (b) Pole figure representation of the previous figures. Dark gray, black and light gray represent the three right, top right and bottom left coarse regions.

From a combination of load relaxation and strain rate change tests (Figure 5-a) a typical Log(stress) vs. Log(strain-rate) curve is obtained. The parameters  $\gamma$  and  $\sigma^*$  can be estimated from these curves. They can be correlated to those obtained from the microstructure. The load relaxation results show a very minimal work hardening behavior at higher strains for the superplastic material. The results however show a slight variation in  $\gamma$  as the material strains. Figure 5-b presents the corresponding misorientation distribution for different strain levels. This result shows that as the material deforms, there is a shift from low angle boundaries of less than 5 degrees to high angle boundaries of higher than 40 degrees. The volume fraction of low angle grain boundaries drop from 40% to 12%. All these results show that a fraction of the grains remain as low angle grain boundaries even at a strain of 660% (10-12%).

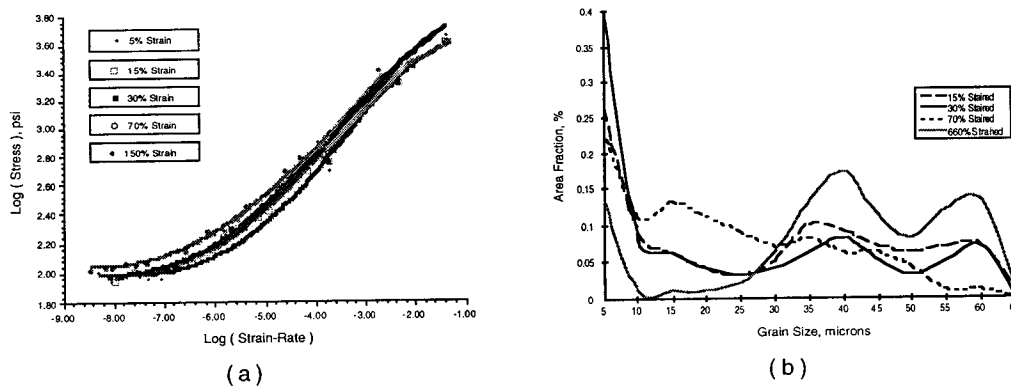


Figure 5- Composite of Test Results for Al-Li 8090 at (a) Load relaxation and strain rate change test at 516 °C and (b) Misorientation histogram for Al-Li-8090 at Four Strain Levels.

The full analysis of the grain boundaries (Coincidence Site Lattice-CSL information) will be presented elsewhere. It is however interesting to observe how the grain size distribution varies for the different grain boundary criteria (Figure 6 and 7). Only the low (15%) and high strain (660%) results are presented with the realization that such a comparison may not be adequate to draw a definite conclusion on the nature of these boundaries. Note that the 3 degree boundary criteria also includes the higher angle boundaries. As a result, the distribution for such a criteria shows a very fine grain microstructure and is favored towards the smaller grains. When the higher angle criteria is chosen the distribution is favored towards the larger angle boundaries. For larger strains, the distribution is the same regardless of the grain boundary criteria used.

#### CONCLUSION

An investigation of the nature of the grain boundaries in an Al-8090 superplastic material is presented and an attempt has been made to produce a unified model for superplasticity. The model accounts for deformation in superplastic and non-superplastic regions. Orientation Imaging Microscopy was used to obtain various microstructural parameters such as grain boundary misorientation. The microstructural changes which occurred during superplastic deformation is discussed in terms of the mechanical property (strain rate stress relationship) and grain size and misorientation angle distribution. The results show that the investigation of the OIM results should be performed with proper attention to the type of criteria used to define grain boundaries. It is also very clear that parameters such as grain size should be redefined in terms of their distribution and the nature of such distribution can determine the nature of superplasticity.

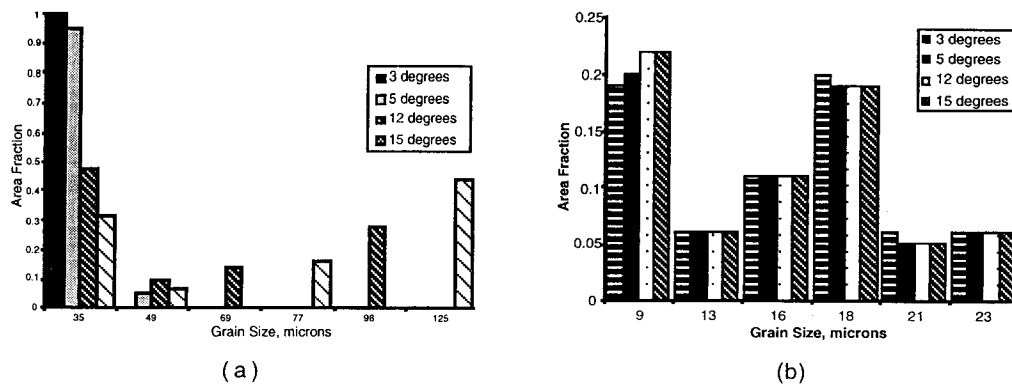


Figure 6- Grain size distribution for two specimens at a) initial stage of superplastic deformation,  $\epsilon=15\%$ , b) final stage of superplastic deformation  $\epsilon= 660\%$ .

#### ACKNOWLEDGEMENTS

This work was supported by a grant from the NASA-FAMU Center for Nonlinear and Nonequilibrium Aerospace (CENNAS) at the National High Magnetic Field Laboratory and the Center for Materials Research and Technology (MARTECH) at the Florida State University.

#### REFERENCES

- [ 1 ] B. P. Kashayap, A. Arieli, and A. K. Mukherjee, "Review of microstructural aspects of superplasticity," *Journal of Materials Science*, vol. 20, pp. 2661-2686, 1985.
- [ 2 ] A. K. Ghosh and C. H. Hamilton, "Influence of Material Parameters and Microstructure on Superplastic Forming," *Metall. Trans.*, vol. 13A, pp. 733-743, 1982.
- [ 3 ] A. K. Mukherjee, "Deformation Mechanisms In Superplasticity," *Annual Review Material Science*, vol. 9, pp. 191-217, 1979.
- [ 4 ] M. F. Ashby and R. A. Verrall, "Diffusion-Accommodated Flow and Superplasticity," *Acta Metallurgica*, vol. 21, pp. 149-163, 1973 February.
- [ 5 ] T. G. Langdon, "The Physics of Superplastic Deformation," *Materials Science and Engineering*, vol. A137, pp. 1-11, 1991.
- [ 6 ] P. N. Kalu and T. R. McNelley, "Investigation of the Deformation Mechanisms in Superplastic Al-Mg Alloys by Microtexture technique," presented at Proceeding of Light-Weight Alloys for Aerospace Applications II, 1991.
- [ 7 ] J. A. Venebles and C. J. Harland, in *Phil. Mag.*, vol. 27, 1973, pp. 1193-1200.
- [ 8 ] A. Ball and M. M. Hutchinson, *Journal of Metal Science*, vol. 3, pp. 1, 1969.
- [ 9 ] S. I. Wright, B. L. Adams, and K. Kunze, "Application of a new Automatic Lattice Orientation Measurement Technique to Polycrystalline Aluminum," *Materials Science and Engineering*, vol. A160, pp. 229-240, 1993.
- [ 10 ] E. W. Hart, "A Theory For Flow of Poly- crystals," *Acta Metallurgica*, vol. 15, pp. 1545-1549, 1967 September.
- [ 11 ] B. Baudalet, "A composite model for superplasticity," *Materials Science and Engineering*, 1995.
- [ 12 ] F. Boeshaghi and H. Garmestani, "Rheological Modeling of Superplasticity," presented at Proceeding of the 32nd annual conference of SES, 1995.
- [ 13 ] K. Z. Baba-Kishi and D. J. Dingley, "Backscatter Kikuchi Diffraction in the SEM for Identification of Crystallographic Point Groups," *Scanning*, vol. 11, pp. 305-312, 1989.
- [ 14 ] H. Garmestani, P. N. Kalu, and D. Dingley, presented at Proceeding of the Light Weight Alloys for Aerospace Applications III, 124th Annual Meeting of TMS, 1995, Feb 12-16.
- [ 15 ] H. Garmestani and P. N. Kalu, "Taken from an unpublished research," , 1996.